Nano World Journal

https://doi.org/10.17756/nwj.2023-s3-161

Research Article

Open Access

Investigating the Influence of Machining Parameters on Surface Roughness in AA2024/n-SiC Metal Matrix Composites Using Cryogenic Coolant

Kulathuraan Kavu[1], Adil Ahmed Sirajuddin[2], Hemanth Raju Thippeswamy[3], Vikrant Ganvir[4], Rajasekaran Saminathan[5], Anantha Padmanabham Koti Chakrapani[6] and Satishkumar Palanisamy[7*]

[1]*Department of Physics, Arulmigu Palaniandavar College of Arts and Culture, Palani, Tamil Nadu, India*

[2]*Department of Mechanical Engineering, KNS Institute of Technology, Bengaluru, India*

[3]*Department of Mechanical Engineering, New Horizon College of Engineering, Bangalore, India*

[4]*Department of Applied Physics, Yeshwantrao Chavan College of Engineering, Nagpur, India*

[5]*Department of Mechanical Engineering, College of Engineering, Jazan University, Saudi Arabia*

[6]*Department of Mechanical Engineering, Don Bosco Institute of Technology, Bengaluru, India*

[7]*Department of Mechanical Engineering, Rathinam Technical Campus, Coimbatore, Tamil Nadu, India*

***Correspondence to:**
Satishkumar Palanisamy
Department of Mechanical Engineering,
Rathinam Technical Campus,
Coimbatore, Tamil Nadu, India.
E-mail: sp.sathishkumar10@gmail.com

Received: July 31, 2023
Accepted: November 01, 2023
Published: November 03, 2023

Citation: Kavu K, Sirajuddin AA, Thippeswamy HR, Ganvir V, Saminathan R, et al. 2023. Investigating the Influence of Machining Parameters on Surface Roughness in AA2024/n-SiC Metal Matrix Composites Using Cryogenic Coolant. *NanoWorld J* 9(S3): S907-S914.

Published by United Scientific Group

Abstract

Metal matrix composite (MMC) is one type of composite that has seen a significant increase in popularity in recent years. The growing breadth of MMC applications justifies further investigation of their machinability. Rapid machining methods are also utilized to increase production speed. The goal of this research was to discover if higher cutting forces resulted from rougher surfaces in high-speed AA2024/n-SiC composites. The CO_2 cryo coolant and MMC fabricated from AA2024/n-SiC, which is 16% SiC, to reach cutting rates of 2700 m/min. The experiment also used a 5-tiered central composites design. Cutting forces rise by 4 - 9% points when using CO_2 cryogenic coolants, but surface roughness (SR) rises by 18 - 24% points. With coolant, feed rates below 0.12 mm/tooth, cutting speeds over 2300 m/min, and depth of cut (DOC) between 1.0 and 1.5 mm produce the smoothest surfaces.

Keywords

Surface roughness, Cryogenic coolant, SiC, Cutting speed, MMCs, Feed rate

Introduction

For over twenty years, demand for MMCs has grown steadily [1]. Particulate MMCs with changed physical and improved mechanical properties appealing for structural and electrical domain can be manufactured cheaply by incorporating ceramic particles into light alloys, a unique approach [2]. According to the researchers, MMCs are finding applications in the fields of aerospace, electronics, and even medicine. According to MMC-assess, the excellent ductility, lower density, and greater corrosion resistance of aluminum and magnesium make them two common metal matrix used in MMCs [3]. With their improved mechanical and physical qualities, aluminum alloys provide new opportunities for numerous industrial applications where lightweight design is essential [4]. Reinforcing ceramic particles are typically comprised of alumina (Al_2O_3) and siC (n-SiC) and exist in a wide range of shapes and sizes [5]. The superior mechanical properties and ready availability of Aluminum composites with Alumina and n-SiC reinforcement particles have led to their widespread use. Aluminum MMCs are desirable for structural uses because of their excellent strength-to-weight and stiffness-to-weight ratios. But the high price of composite production is a serious problem [6].

While high-speed machining (HSM) has been the subject of fewer studies,

composite material machining has been studied extensively. The authors [7] refined the machining parameters for turning Al-n-SiC-Gr composites. The researchers [8] also discovered that the machinability of the final composites was improved by increasing the n-SiC-Gr mass fraction. While milling AA2024/n-SiC MMCs at high speeds (600 - 1200 m/min) with PCD equipment, the author [9] studied the impact of cutting forces. Both feed rate and radial DOC contribute to a rise in cutting forces. However, it has been demonstrated that increased cutting speed decreases cut force [10]. For the reinforcement, cutting forces grow with both larger and smaller particles. 10 holes were drilled into n-SiCp/aluminum composites by author [11] to test the effectiveness of diamond-coated drill bits.

The most significant wear mechanisms in diamond tools were found to be mechanically induced abrasion and heat graphitization, as observed during drilling of Cu-containing n-SiCp/aluminum composites. Author [12] found that machining parameters, specifically the radius of the diamond sphere, affect surface qualities. According to their findings [13], SR and flaws can be drastically reduced with slide burnishing using a 25% volume percentage of n-SiC particles. The SR of AA2024/n-SiCp MMC was studied by adjusting the turning factors (cutting speed, DOC, and feed rate) using WC inserts. Scientists proved that preheated temperature, feed rate, and DOC all impact the cutting speed, DOC, and feed rate forces exerted beneath the machined surface [14]. When milling in a dry machining environment, greater milling speeds and smaller cutting feeds produced the highest surface quality. The SR of aluminum Mg_2Si composites with a 25% aluminum content was studied by the author [15]. Further investigation led to the formulation of an equation that predicts the SR of products as a function of processing parameters with 95% accuracy [16].

Surprisingly little research has been done on force-cutting composites in the last few years [17], despite the obvious benefits of HSM. HSM of a AA2218 T6 matrix/n-SiC with 15% particulate was studied to determine its impacts. Cutting speed (1100 - 2700 m/min), feed rate and depth of cut (0.5 - 2.5 mm) were all investigated for their effects on SR (0.03 - 0.15 mm per tooth). All the devices featured force measurements to help scientists get a fuller picture of machining behaviour [18]. Mechanical qualities and their relation to CO_2 cooling have been studied. The dimensions of the answers may be correlated with the two sets of inputs after the factors governing them were understood [19]. Five levels, -2, -1, 0, +1, and +2 were determined for each numerical input parameter in this process. Experiments measured quantitative factors including DOC, feed rate and cutting speed. Consumption of coolants was coded as a categorical variable, with a value of +1 when CO_2 was available and a value of -1 when conditions were dry. By adjusting three fixed numerical parameters over five tiers and two cooling conditions, 40 design points were investigated [20]. In this study, DOE was used to evaluate the impact of various machining parameters on SR, both with and without the use of a cooling process. Fast milling of AA2024/ n-SiC MMCs was also recommended, along with the optimal machining settings.

Experimental Setup

AA2024-T6 alloy was used to test MMC samples. The wettability was improved by using n-SiC particles. Particle rebound and conglobation in slag were both avoided by setting the reinforcing particle weight percentage at 16 wt %. The low price of the vortex casting method aided the fabrication of composites. The author [21] describes how the melting was performed in a resistance furnace with an argon environment and a graphite crucible.

The matrix alloy was weighed out and placed in the crucible before the furnace was ignited. The furnace was heated to 725 °C and kept there until all the matrix material had melted. To improve particle absorption, the temperature was decreased to 675 °C. The pre-wetting of the particles was improved by the addition of 0.5% by weight of magnesium to the mixture. For two h at 1000 °C, n-SiC particles had their composites oxidized, and then they were fed steadily into a graphite impeller that had been preheated to 675 °C. The mixed slurry's flowability was improved by heating it to a height of 725 °C. Researchers swirled for an additional five min after adding all the particles. After the sludge was thoroughly mixed, it was poured into a preheated steel die [22]. After the slurry had been compacted to a solid state at a pressure of 40 MPa, the die was taken out of the press. There were also several standard samples included, their profiles were 40 mm^2 × 60 mm^2. Table 1 displays the AA2024 chemical compositions.

The sample was machined in a single pass (64 mm) because the diameter of the tool (68 mm) was greater than the width of sample (100 mm). The experiment was set up with a five-stage Central composite Design (CCD). Inputs and their corresponding intensities are tabulated in table 2. With the current state of technology, the maximum machining speed can reach 2700 m/min, while the minimum machining speed can reach 1100 m/min. In both dry and CO_2 machines, the focal point selection from the CCD determines the Cutting Speed (1900 m/min), DOC (1.5 mm) and Feed rate (0.09 mm/tooth). Dry machines, as well as machine using CO_2 cryogenic coolant, were also employed. Figure 1 shows that the blade's cutting length is 22 mm. Cutting force is highest in the first stage, when the tool is making full contact with the material being cut.

The underside quality of machined components was evaluated using SR (Ra) measurements. To ensure the

Table 1: AA2024 chemical compositions.

Material	Ti	Si	Cu	Fe	Mn	Cr	Mg	Zn	Al
Wt%	0.2	1	3.8 - 4.9	1	03 - 0.9	0	1.2 - 1.8	0.3	Bal

Table 2: Inputs and levels of the CCD.

Input parameters	Levels				
Cutting speed (m/min)	1100	1500	1900	2300	2700
DOC (mm)	0.5	1	1.5	2	2.5
Feed rate (mm/tooth)	0.03	0.06	0.09	0.12	0.15
Coolant	Dry	CO_2	-	-	-

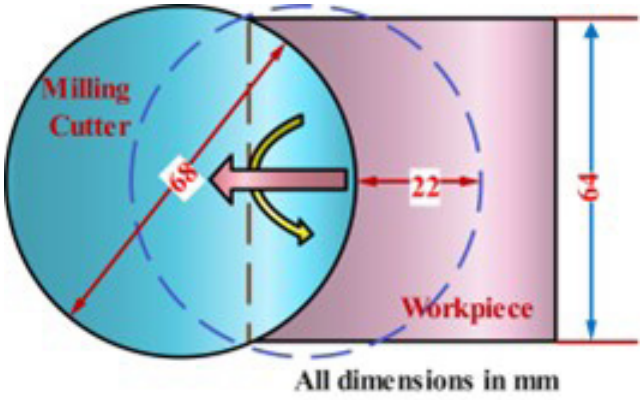

Figure 1: Complete material contact with the cutting tool.

utmost precision, we measured the SR in all four orthogonal directions three times at each of the three locations. Finally, Ra was calculated for each specimen by averaging the values from all measurement sites. Figure 2 depicts the setup used in the experiments.

Results and Discussion

Cutting speed, feed rate, DOC, and coolant conditions were studied as they pertained to the SR of the cutting parameters during face milling. According to the parameters of the CCD, forty tests will be carried out, with a special emphasis on the centers in twelve of them. The CCD algorithms are responsible for this configuration. All the measurements taken throughout the experiment are shown in table 3.

To characterize the forces while accounting for input variability, the 2FI model is presented. Four additional equivalences are shown in table 4 that can be inferred from model 1. The linear link between cutting speed, coolant, and force is evident from these equations.

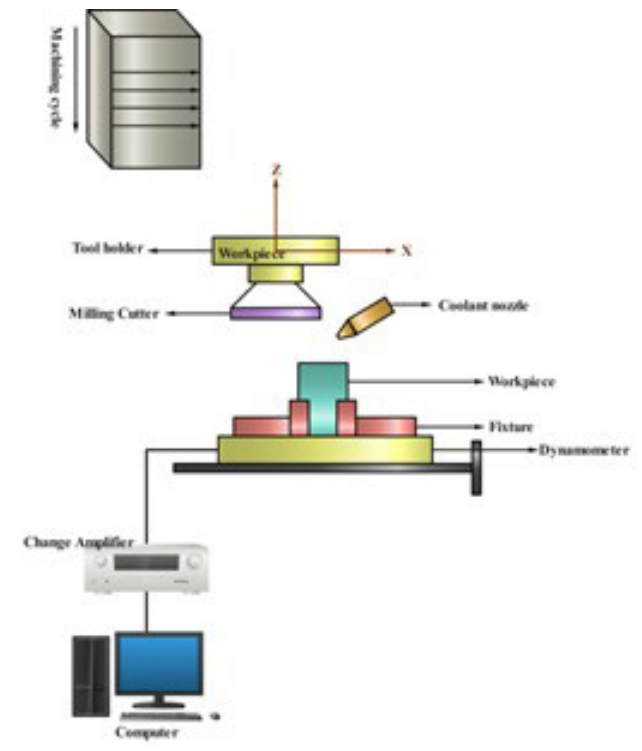

Figure 2: Schematic of experimental setup.

According to equation 3 in table 3, the effect of DOC difference on dry mode middle point forces is displayed in figure 3. The tougher unformed chip profile is responsible for the greater tool resistance.

The dry mode and the centre of the graph in figure 4 represent the solution to Equation 2. The coolant is represented by a -1, the DOC by a zero, the feed rate by a zero, and the cutting speed by a value between ± α and inclusive. The impact of varying cutting speeds on the resulting cutting forces can be investigated in this setting. Increasing the cutting speed, as displayed in figure 4, decreases the machining forces. Because HSM causes the workpiece to soften thermally, less force is needed to machine the material. However, faster cutting rates reduce the likelihood of edge development. The constant for

Table 3: Experimental design.

S. No	Cutting speed	Depth of cut	Feed rate	Coolant	Force N	SR (µm)
1	1500	1	0.06	Dry	190	0.353
2	2300	1	0.06	Dry	192	0.28
3	1900	1.5	0.15	Dry	259	0.402
4	1900	1.5	0.09	Dry	266	0.576
5	1500	2	0.12	CO_2	355	0.364
6	2700	1.5	0.09	CO_2	201	0.3
7	1500	1	0.06	CO_2	195	0.296
8	1900	1.5	0.03	Dry	205	0.294
9	2300	1	0.12	Dry	183	0.482
10	2300	2	0.06	CO_2	282	0.4
11	1900	1.5	0.09	Dry	236	0.625
12	1900	0.5	0.09	Dry	190	0.327
13	2300	1	0.06	CO_2	202	0.257
14	1900	1.5	0.09	CO_2	270	0.485
15	1900	1.5	0.09	CO_2	265	0.474
16	1900	1.5	0.15	CO_2	255	0.401
17	1900	1.5	0.09	Dry	250	0.581
18	1900	1.5	0.09	Dry	259	0.562
19	1900	1.5	0.09	CO_2	301	0.582
20	1500	2	0.06	Dry	273	0.454
21	2300	2	0.06	Dry	250	0.519
22	1900	1.5	0.09	CO_2	252	0.485
23	2300	2	0.12	CO_2	288	0.512
24	1900	1.5	0.09	Dry	263	0.528
25	1500	2	0.09	Dry	347	0.42
26	1000	1.5	0.09	Dry	311	0.789
27	2300	2	0.12	Dry	275	0.57
28	2700	1.5	0.09	Dry	231	0.359
29	1000	1.5	0.09	CO_2	329	0.648
30	1500	2	0.06	CO_2	288	0.397
31	1900	1.5	0.09	CO_2	279	0.444
32	1900	0.5	0.09	CO_2	119	0.296
33	1900	1.5	0.09	CO_2	297	0.478
34	1900	2.5	0.09	Dry	377	0.694
35	1900	2.5	0.09	CO_2	359	0.442
36	1500	1	0.12	Dry	211	0.534
37	1900	1.5	0.03	CO_2	209	0.256
38	1500	1	0.03	CO_2	228	0.45
39	2300	1	0.03	CO_2	203	0.364
40	1900	1.5	0.09	Dry	280	0.556

Table 4: Force and input factor mathematical modelling.

Input parameters	Equation number	Eqn. of input parameter and force
---	1	$F = 272.62 - 23.72\ A + 64.14\ B + 11.1C + 7.21D - 12.24 - 11.53\ B^2 - 14.05C^2$
Cutting force	2	$F = (263.62 + 63.14\ B + 17.1C + 9.21D - 13.24\ B^2 - 14.05C^2) - (22.67 - 12.69C)A$
Depth of cut	3	$F = (263.62 - 23.72\ A + 17.1C + 9.21D - 12.69AC - 14.05C^2) + 63.14\ B - 13.24\ B^2$
Feed rate	4	$F = (263.62 - 23.72\ A + 63.14B + 9.21D - 13.24\ B2) + (16.1 - 12.69\ A)C - 14.05C^2$
Coolant	5	$F = (263.62 - 23.72\ A + 63.14\ B + 16.1C - 13.24AC - 12.53\ B^2 - 14.05C^2) + 9.21D$

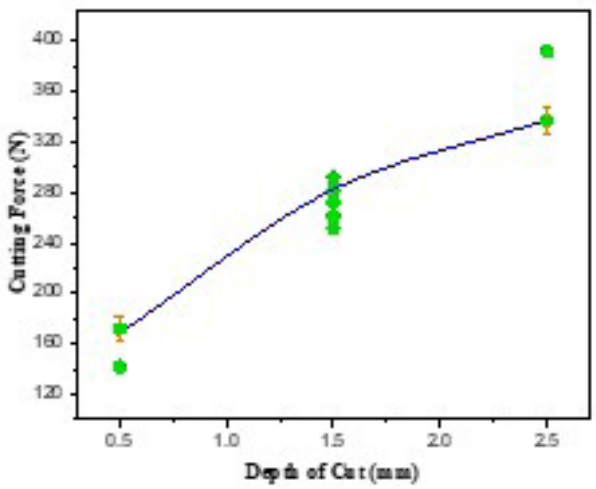

Figure 3: Effect of depth of cut on cutting force.

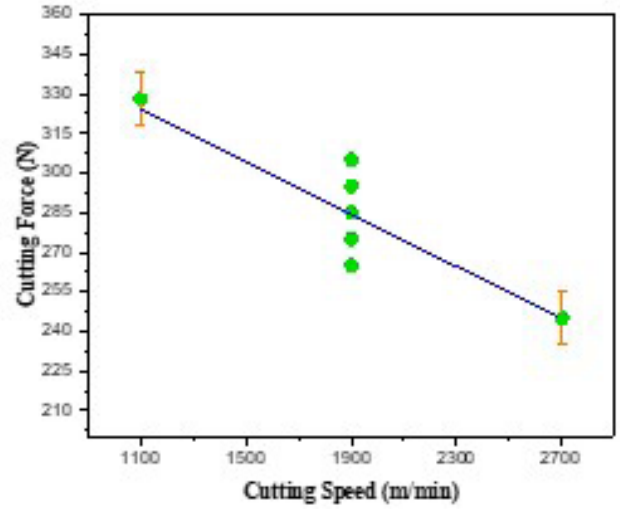

Figure 4: Evaluation of cutting force and cutting speed at middle point.

cutting speed includes a variable proportional to the feed rate, hence the relationship between cutting speed and cutting force has a non-uniform slope (Figure 5). The rate at which machine forces are reduced is displayed in figure 4 to be a function of the feed rate and cutting speed. Machining forces increase with a higher feed rate, but cutting speeds have a much greater effect on the overall force requirement. When both are raised, the force is diminished.

Dry mode cutting forces versus feed rate are depicted in figure 6. It has been discovered that the forces first increase when the feed rate is increased, before stabilizing off. Aluminum matrix with SiC particles that are 0.05 to 0.07 mm in size. Author [23] discovered that when working with MMCs, greater forces are required since the particles must be fractured throughout the machining development. If both the chip and the particle size are kept the same, the force improvement is maximized. After that point, it will have less of an effect because there may already be whole particles in

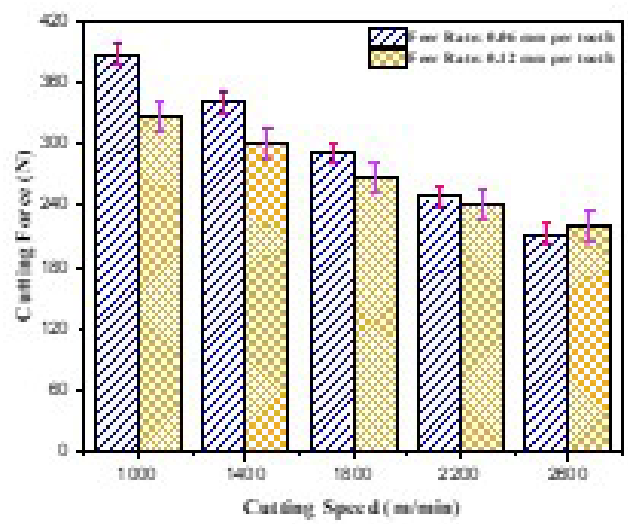

Figure 5: Feed rate versus cutting speed and cutting force.

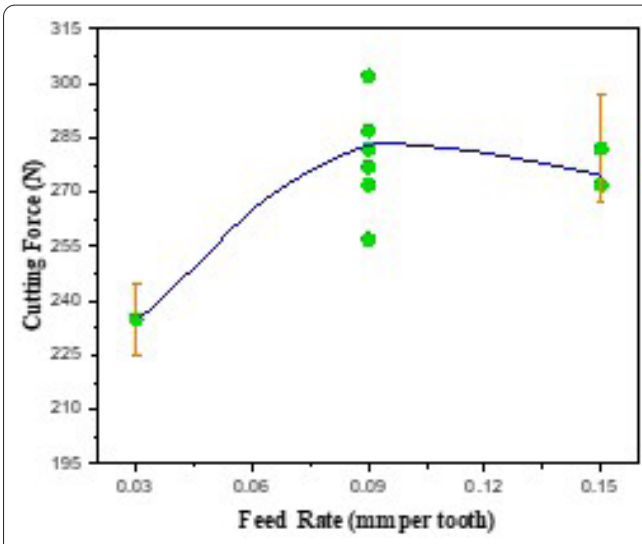

Figure 6: Evaluation of cutting force and feed rate at middle point.

circulation, reducing the possibility of particle splitting. In a feed rate-force graph, the force increase is greatest when the rate of feed is proportional to the size of the particles. When feed rates are lowered, cutting speeds are raised, lowering the peak of the curve. Figure 7 depicts a few instances of feed rate interactions. Cutting force can be decreased by raising both the cutting speed and feed rate.

The authors [24] shows that as the tool and the workpiece cool, they both harden. If the workpiece is harder than the tool being used, greater machining forces are required. Figure 8 depicts the results of utilizing or not employing a coolant at the apex. The equation 5 was used to determine that, under our experimental conditions, the use of CO_2 coolant raises machining forces by 4.9%.

Parameters used in the experiment and their effect on Ra are shown in table 5. Equations 7 - 10 can be derived from equation 6 by rearranging the terms. Every function becomes nonlinear when subjected to a logarithmic transform. By plotting these functions in the middle of the experimental range, the effects of the input factors on the SR may be more easily visualized. Equation 6 demonstrates that coolant has no impact on the SR because the SR diagram's slope is unrelated to the relationships between the different iterations. The machining behaviour of the workpiece is examined by calculating the forces exerted on it during the process. SR

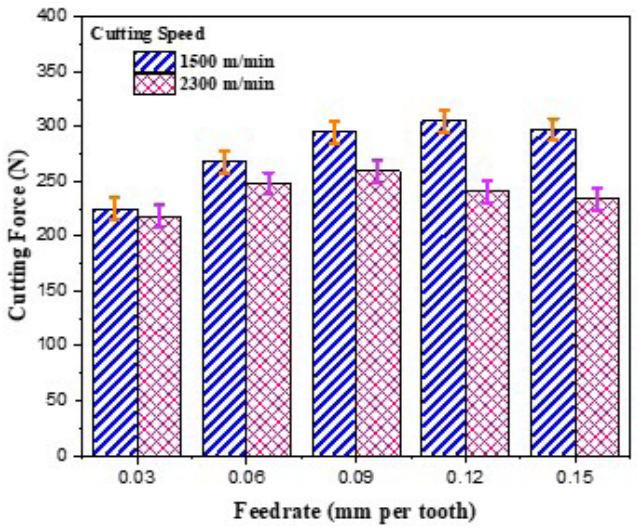

Figure 7: Cutting speed versus cutting force and feed rate.

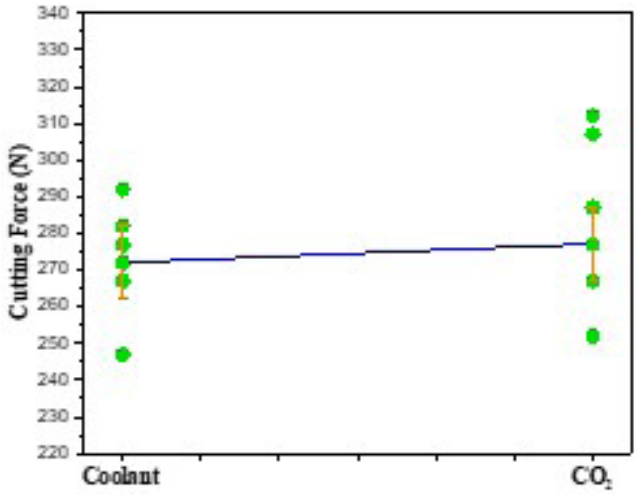

Figure 8: Evaluation of coolant and cutting force.

increases and microcracks form on the machined surface as cutting forces increase [25]. Therefore, increased cutting force may be responsible for the rougher finish. It has been discovered that to achieve a passable surface quality, accurate regulation of DOC, feed rate and cutting speed is essential.

Table 5 shows that the relationship between cutting speed and SR (equation 7) is nearly linear. In the dry mode and close to the geometric centre, the relationship between A and Ra is shown in figure 9. The surface quality improves as the cutting speed is raised because the SR and the centre point are reduced. Researcher [26] found that the lack of reinforcing particles in HSM of raw materials is a foreseeable explanation for poor generated edge on tool at higher speed. This allows scientists to discount the possibility that tool overlap resulted in better surface quality. The authors [4] shows that HSM breaks down the composite material's connection between the base material and reinforcing particles.

When tool and reinforcing particles collide at low speeds, author [27] argues that scratching or pitting occurs because of the ploughing action. A smoother surface may result from the fragmentation of these particles during high-velocity collisions, according to the researchers. SR reduction as a function of feed is displayed in figure 10a, where it is most noticeable in the middle, where the feed is approximately the same as the grain size, and where it gradually reduces at higher or lower feeds. The author [28] suggests increasing the

Table 5: Mathematically modeled SR and input parameters.

Input parameters	Eq. number	Equation of input parameter and SR
---	6	$\log_{10}(SR) = -0.54 - 0.27\,A + 0.098\,B + 0.10C - 0.065D + 0.070AB - 0.079BC - 0.062\,B^2 - 0.100C^2 + 0.26AC^2$
Cutting Speed	7	$\log_{10}(SR) = (-0.54 + 0.098\,B + 0.10C - 0.065D - 0.079BC - 0.053\,B^2 - 0.100C2) + (-0.27 + 0.07\,B + 0.26C^2)A$
Depth of Cut	8	$\log_{10}(SR) = (-0.54 - 0.27\,A - 0.062\,B^2 + 0.10C - 0.065D - 0.100C2 + 0.26AC^2) + (0.098 + 0.070\,A - 0.079C)B$
Feed Rate	9	$\log_{10}(SR) = (-0.54 - 0.27\,A + (-0.100 + 0.A)C^2 - 0.098\,B - 0.065D + 0.070AB - 0.062\,B^2) + (0.10 - 0.079B)C$
Coolant	10	$\log_{10}(SR) = (-0.54 - 0.27\,A + 0.098\,B + 0.10C + 0.070AB - 0.049BC - 0.062\,B2 - 0.100C2 + 0.26AC^2) - 0.065D$

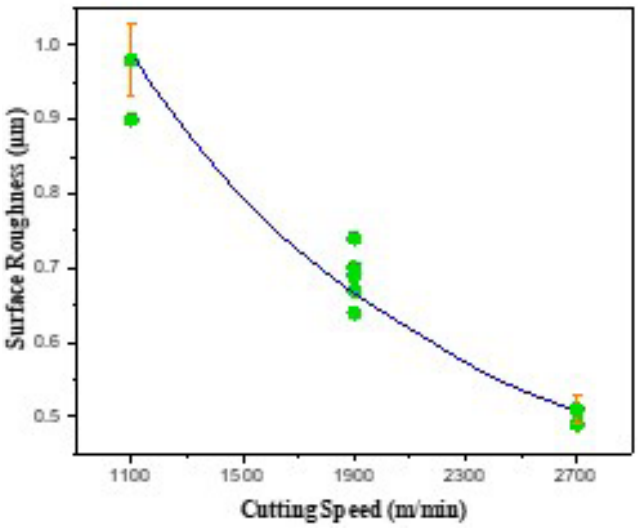

Figure 9: Evaluation of cutting speed and SR at middle point.

machining point temperature to avoid micro fractures caused by the merging of different pore diameters in the workpiece. Higher machine speeds are thought to contribute to the improved surface quality by honing and burnishing the tool edges. This technique works best when the feed rate is directly proportionate to the particle size. Figure 10b demonstrates that the SR is a multiplicative function of the DOC. A flatter cutting speed SR diagram is the result of increased machine vibration with increasing cut depth during HSM. This squares with the results of investigations on stability lobes in the literature of HSM vibrational studies [29].

Figure 11 and equation 8 demonstrate that the DOC impacts both the middle-to-edge and dry-mode SR. It is demonstrated experimentally that there is a maximum allowable roughness at the cut depth. The SR increases as the DOC rises because of the higher cutting pressures. The recent smoothing of the surface is probably due to SiC particles in the underlying metal's matrix. Figure 12a depicts the SR equation for a dry cut across the centre as a function of cutting speed.

As the peak of the DOC graph moves further into the hole, cutting faster reduces SR. This is because the cutting tool loses more vibrational energy the deeper it goes [30]. Figure 12b illustrates the reciprocal effect of DOC on feed rate and the RS equation. As the feed rate rises, the graph's peak will approach the horizontal. Increases in cutting pressure can be traced back to the adoption of a chip profile that is too high. As a result, the cutting depth at which the graph's peak occurs decreases when the feed rate is increased.

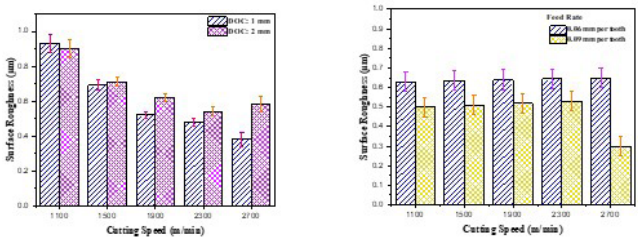

Figure 10: (a) DOC **(b)** Feed rate on SR and cutting speed.

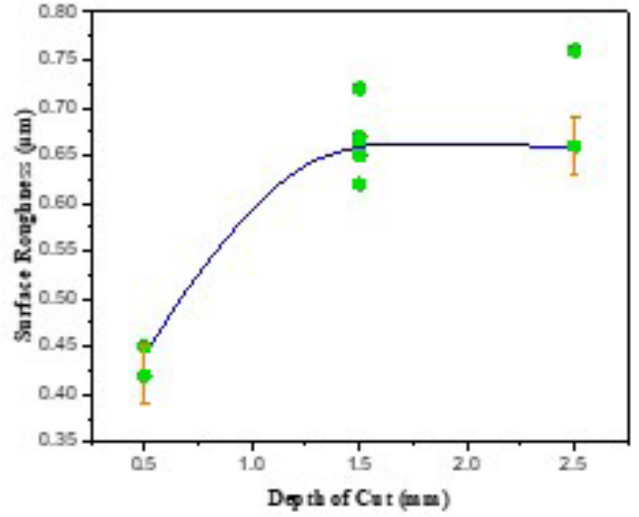

Figure 11: Evaluation of DOC and SR at middle point.

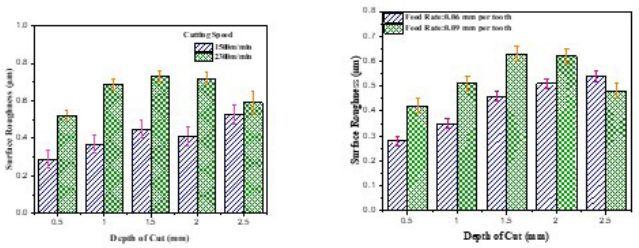

Figure 12: (a) Cutting speed and **(b)** Feed rate on DOC and SR.

Figure 13 depicts the relationship between the dry mode SR (Equation 9) and the feed rate. There is a maximum value for the DOC-SR equation within the experimental range. When machining non-composite materials, increasing the chip width almost never results in a smoother surface. However, as Grzesik points out, the SR will also rise significantly if additional feed is supplied to each tooth. These results suggest that as feed rate magnitude gets closer to grain size, machining forces increase alongside SR.

When the cutting pressure is increased, the SR also rises

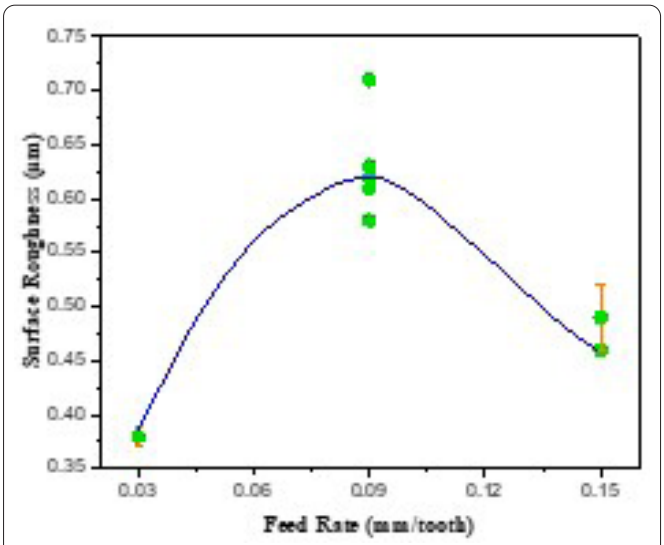

Figure 13: Evaluation of feed rate and SR at middle point.

until it plateaus at the DOC. In both wet and dry cutting, the SR equation is impacted by the feed rate and cutting speed. Surface smoothness after cutting is typically determined by the cutting speed. As cutting speeds rise due to burnishing and tool honing, SR decreases (Figure 14a), moving the highest point to the low location. As can be shown in figure 14b, DOC influences the feed rate-SR both in dry mode and at the midpoint. As cutting depth increases, a lower peak appears in the feeding diagram. That's because the chip profile broadens with increasing DOC and feed rate, so higher cutting speeds get you to the critical cutting force range faster.

Effect of coolant

Coolant has a significant effect on SR, as shown in figure 15. Due to CO_2's ability to maintain a consistent hardness and so reduce tool wear, SR rises by 18% to 24% when used as a coolant (Equation 10).

Conclusion

This study investigates the response of AA2024/n-SiC composites to high-speed machine, where reinforcement particles account for 16% of the total weight. Because AMCs contained hard SiC particles, describing their machining performance was complex. These are the most significant results.

Raised feed rates (0.03 - 0.15 mm/tooth) and DOC (0.5 - 2.5 mm) increase SR. Lowest machining forces are achieved with high cutting speed, a high feed rate, and a low DOC. It shouldn't take more than 200 N of machine force to achieve cutting speeds of more than 2300 m/min and feed rates of less than 1 mm/min. The machine force also increases by 4 - 9% when using CO_2 as the coolant.

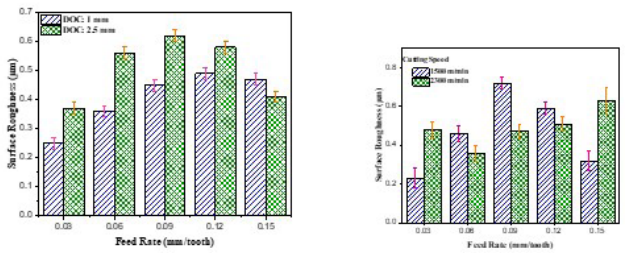

Figure 14: (a) DOC and **(b)** Cutting speed on SR and feed rate.

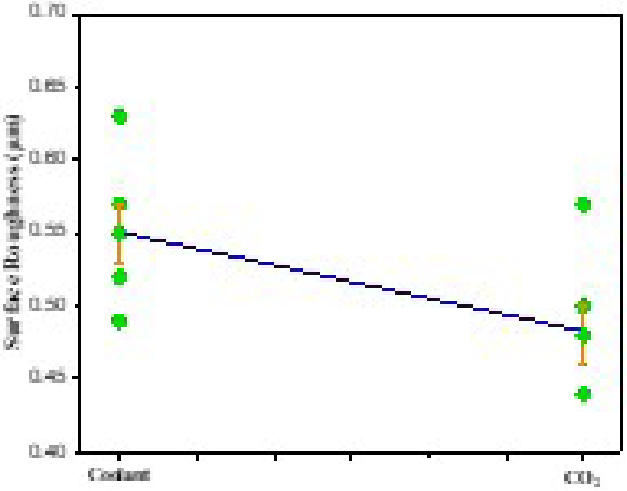

Figure 15: Evaluation of different coolant on SR.

SR of less than 0.25 m can be achieved during dry machining of AA2024/n-SiC by maintaining a cutting speed of more than 2300 m/min, a DOC of less than 1 mm, and a feed rate of less than 0.06 mm/tooth (the size of nano SiC particles). Using CO_2 as a coolant also allows for an increase in SR of 18 - 24%.

A rise in cutting speed does not necessarily result in a higher quality product during MMC machining. Surprisingly, SR rises with increasing cutting speed for DOC values greater than 2 mm and feed rates as higher as 0.09 mm/tooth and as low as 0.06 mm/tooth. An adequate SR is predicted when the feed rate is proportionate to the n-SiC and the cutting speed is greater than the DOC.

Acknowledgements

None.

Conflict of Interest

None.

References

1. Lakshmanan S, Kumar MP, Dhananchezian M. 2023. Optimization of turning parameter on surface roughness, cutting force and temperature through TOPSIS. *Mater Today Proc* 72: 2231-2237. https://doi.org/10.1016/j.matpr.2022.09.209
2. Singh NK, Singh Y, Sharma A, Paswan MK, Singh VK, et al. 2021. Performance of CuO nanoparticles as an additive to the chemically modified *Nicotiana tabacum* as a sustainable coolant-lubricant during turning EN19 steel. *Wear* 486: 204057. https://doi.org/10.1016/j.wear.2021.204057
3. Dhananchezian M, Rajashekar G, Narayanan SS. 2018. Study the effect of cryogenic cooling on machinability characteristics during turning duplex stainless steel 2205. *Mater Today Proc* 5(5): 12062-12070. https://doi.org/10.1016/j.matpr.2018.02.181
4. Ramesh B, Kumar SS, Elsheikh AH, Mayakannan S, Sivakumar K, et al. 2022. Optimization and experimental analysis of drilling process parameters in radial drilling machine for glass fiber/nano granite particle reinforced epoxy composites. *Mater Today Proc* 62: 835-840. https://doi.org/10.1016/j.matpr.2022.04.042
5. Manikandan R, Ponnusamy P, Nanthakumar S, Gowrishankar A, Balambica V, et al. 2023. Optimization and experimental investigation on AA6082/WC metal matrix composites by abrasive flow machining process. *Mater Today Proc* 2023. https://doi.org/10.1016/j.matpr.2023.03.274
6. Srinivasan R, Karunakaran S, Hariprabhu M, Arunbharathi R, Suresh S, et al. 2023. Investigation on the mechanical properties of powder metallurgy-manufactured AA7178/$ZrSiO_4$ nanocomposites. *Adv Mater Sci Eng* 2023: 1-11. https://doi.org/10.1155/2023/3085478
7. Khatai S, Sahoo AK, Kumar R, Panda A. 2023. Recent research progress on various cooling and lubrication techniques used in sustainable hard machining: a comprehensive review. *J Proc Mech Eng* 2023: 09544089231169655. https://doi.org/10.1177/09544089231169655
8. Österreicher JA, Nebeling D, Grabner F, Cerny A, Zickler GA, et al. 2023. Secondary ageing and formability of an Al-Cu-Mg alloy (2024) in W and under-aged tempers. *Mater Des* 226: 111634. https://doi.org/10.1016/j.matdes.2023.111634

9. Chakravarthy VK, Rajmohan T. 2020. Analysis of power consumption in the drilling of nano SiC reinforced aluminium matrix composites. *IOP Conf Ser Mater Sci Eng* 954(1): 012038. https://doi.org/10.1088/1757-899X%2F954%2F1%2F012038
10. Gupta MK, Niesłony P, Korkmaz ME, Królczyk GM, Kuntoğlu M, et al. 2023. Potential use of cryogenic cooling for improving the tribological and tool wear characteristics while machining aluminum alloys. *Tribol Int* 183: 108434. https://doi.org/10.1016/j.triboint.2023.108434
11. Gupta MK, Korkmaz ME, Sarıkaya M, Krolczyk GM, Günay M, et al. 2022. Cutting forces and temperature measurements in cryogenic assisted turning of AA2024-T351 alloy: an experimentally validated simulation approach. *Measurement* 188: 110594. https://doi.org/10.1016/j.measurement.2021.110594
12. Satishkumar P, Mahesh G, Meenakshi R, Vijayan SN. 2021. Tribological characteristics of powder metallurgy processed Cu-WC/SiC metal matrix composites. *Mater Today Proc* 37: 459-465. https://doi.org/10.1016/j.matpr.2020.05.449
13. Elsheikh AH, Shanmugan S, Muthuramalingam T, Thakur AK, Essa FA, et al. 2022. A comprehensive review on residual stresses in turning. *Adv Manuf* 1-26. https://doi.org/10.1007/s40436-021-00371-0
14. Satyanarayana G, Narayana KL, Rao BN. 2021. Incorporation of Taguchi approach with CFD simulations on laser welding of spacer grid fuel rod assembly. *Mater Sci Eng* 269: 115182. https://doi.org/10.1016/j.mseb.2021.115182
15. Satishkumar P, Krishnan GG, Seenivasan S, Rajarathnam P. 2023. A study on tribological evaluation of hybrid aluminium metal matrix for thermal application. *Mater Today Proc* 81: 1097-1104. https://doi.org/10.1016/j.matpr.2021.04.389
16. Chakravarthy VK, Rajmohan T, Vijayan D, Palanikumar K. 2023. Application of grey-ANFIS system to optimize the drilling characteristics of nano SiC reinforced Al matrix composites. *Int J Interact Design Manuf* 17(6): 3117-31131. https://doi.org/10.1007/s12008-023-01328-2
17. Jia Y, Su R, Wang L, Li G, Qu Y, et al. 2023. Study on microstructure and properties of AA2024-T6I4 with deep cryogenic treatment. *Trans Indian Inst Metals* 76(3): 741-748. https://doi.org/10.1007/s12666-022-02764-6
18. Satishkumar P, Rakesh AI, Meenakshi R, Murthi CS. 2021. Characterization, mechanical and wear properties of Al6061/Sicp/fly ashp composites by stir casting technique. *Mater Today Proc* 37: 2687-2694. https://doi.org/10.1016/j.matpr.2020.08.530
19. Dharmaiah G, Sridhar W, Balamurugan KS, Chandra Kala K. 2022. Hall and ion slip impact on magneto-titanium alloy nanoliquid with diffusion thermo and radiation absorption. *Int J Ambient Energy* 43(1): 3507-3517. https://doi.org/10.1080/01430750.2020.1831597
20. Abushanab WS, Moustafa EB, Harish M, Shanmugan S, Elsheikh AH. 2022. Experimental investigation on surface characteristics of Ti6Al4V alloy during abrasive water jet machining process. *Alex Eng J* 61(10): 7529-7539. https://doi.org/10.1016/j.aej.2022.01.004
21. Vidyasagar CS, Karunakar DB. 2020. Characterization of mechanical properties and microstructures of spark plasma sintered and cryo-rolled AA2024–Y composites. *Trans Nonferrous Met Soc China* 30(6): 1439-1451. https://doi.org/10.1016/S1003-6326(20)65309-2
22. Adin MŞ. 2023. Machining aerospace aluminium alloy with cryo-treated and untreated HSS cutting tools. *Adv Mater Proc Technol* 1-26. https://doi.org/10.1080/2374068X.2023.2273035
23. Niu QL, Jing L, Yu Z, Li CP, Qiu XY, et al. 2022. Experimental study on cryogenic milling performance of SiCp/Al composites with liquid nitrogen. *Mach Sci Technol* 26(1): 1-7. https://doi.org/10.1080/10910344.2021.1971707
24. Ghoreishi R, Roohi AH, Ghadikolaei AD. 2018. Analysis of the influence of cutting parameters on surface roughness and cutting forces in high speed face milling of Al/SiC MMC. *Mater Res Exp* 5(8): 086521. https://doi.org/10.1088/2053-1591/aad164
25. Ross NS, Manasea Selvin BJ, Nagarajan S, Mashinini PM, Dharmalingam SK, et al. 2023. Novel use of cryogenic cooling conditions in improving the machining performance of Al 8011/nano-SiC composites. *Int J Adv Manuf Technol* 129(3): 1703-1715. https://doi.org/10.1007/s00170-023-12382-1
26. Chakravarthy VK, Rajmohan T, Vijayan D, Palanikumar K. 2022. Sustainable drilling of nano SiC reinforced Al matrix composites using MQL and cryogenic cooling for achieving the better surface integrity. *Silicon* 14(4): 1787-1805. https://doi.org/10.1007/s12633-021-00977-w
27. Swain PK, Mohapatra KD, Swain PK. 2020. Analysis of Al-SiCp nano composite and study of its machining process by using coated carbide tool. *Mater Today Proc* 33: 5566-5572. https://doi.org/10.1016/j.matpr.2020.03.556
28. Kumar S, Sood PK. 2019. Leverage of machining parameters and non-oxide nano ceramic fillers loading on machinability of aluminium matrix based nano-composites. *Mater Res Exp* 6(5): 056516. https://doi.org/10.1088/2053-1591/aaf6fa
29. Swain PK, Mohapatra KD, Swain PK. 2021. Development of Al-SiCp nano composite material and study of its machining process using coated carbide inserts. *Mater Today Proc* 44: 596-602. https://doi.org/10.1016/j.matpr.2020.10.591
30. Kumar SP, Prasada HT. 2021. Investigate the effect of nano cutting fluid and cutting parameters under minimum quantity lubrication (MQL) on surface roughness in turning of DSS-2205. *Mater Today Proc* 43: 3643-3649. https://doi.org/10.1016/j.matpr.2020.09.834